The Compass: Earth Science Journal of Sigma Gamma Epsilon

Volume 87 | Issue 4 Article 1

1-25-2016

Field and Petrographic Analysis of the Indian Peak-Caliente Caldera Complex at Condor and English Canyons in Eastern Nevada

Brennan Brunsvik
Southern Utah University, brennan.brunsvik@gmail.com

Chesley Gale
Southern Utah University, chesley.gale@gmail.com

Mackenzie Cope
Southern Utah University, mackenzcope@gmail.com

Jack Petersen
Southern Utah University, jack.petersen@gmail.com

Sarah Zdanowski
Southern Utah University, sezdanowski@gmail.com

See next page for additional authors

Recommended Citation

Brunsvik, Brennan; Gale, Chesley; Cope, Mackenzie; Petersen, Jack; Zdanowski, Sarah; White, Chapman; Robertson, Westan; Kupfer, Kate; McConkie, Spencer; McDermaid, Stevie; Bruckner, Austin; Yon, Jeff C.E.; Kaiser, Jason; and MacLean, John S. (2015) "Field and Petrographic Analysis of the Indian Peak-Caliente Caldera Complex at Condor and English Canyons in Eastern Nevada," *The Compass: Earth Science Journal of Sigma Gamma Epsilon*: Vol. 87: Iss. 4, Article 1.
DOI: https://doi.org/10.62879/c65933336
Available at: https://digitalcommons.csbsju.edu/compass/vol87/iss4/1

Field and Petrographic Analysis of the Indian Peak-Caliente Caldera Complex at Condor and English Canyons in Eastern Nevada

Authors

Brennan Brunsvik, Chesley Gale, Mackenzie Cope, Jack Petersen, Sarah Zdanowski, Chapman White, Westan Robertson, Kate Kupfer, Spencer McConkie, Stevie McDermaid, Austin Bruckner, Jeff C.E. Yon, Jason Kaiser, and John S. MacLean

FIELD AND PETROGRAPHIC ANALYSIS OF THE INDIAN PEAK-CALIENTE CALDERA COMPLEX AT CONDOR AND ENGLISH CANYONS IN EASTERN NEVADA

Brennan Brunsvik[1], Chesley Gale[2], Mackenzie Cope[3], Jack Petersen[4], Sarah Zdanowski[5], Chapman White[6], Westan Robertson[7], Kate Kupfer[8], Spencer McConkie[9], Stevie McDermaid[10], Austin Bruckner[11], Jeffry C.E. Yon[12], Jason F. Kaiser[13], and John S. MacLean[14]

Department of Physical Sciences
Southern Utah University
351 West University Boulevard
Cedar City, UT 84720 USA

[1] brennan.brunsvik@gmail.com
[2] chesley.gale@gmail.com
[3] mackenzcope@gmail.com
[4] jack.petersen@gmail.com
[5] sezdanowski@gmail.com
[6] chapman.w.white@gmail.com
[7] westanrobertson@gmail.com
[8] stargazer@infowest.com
[9] spencermcconkie@suumail.net
[10] stevie.wm@gmail.com
[11] austinbruckner@suumail.net
[12] jeffry.yon@gmail.com
[13] jasonkaiser@suu.edu
[14] johnmaclean@suu.edu

ABSTRACT

The Indian Peak-Caliente Caldera Complex, or IPCCC, is an ideal site to study how large-scale tectonic forces can influence mineralogy on a local scale. This research was completed and compiled by the Tectonics and Mineralogy classes at Southern Utah University during a joint class field study and subsequent laboratory analyses. During the field trip, the main focuses were to observe caldera collapse relationships and ignimbrite features and to collect samples at Condor Canyon and English Canyon, two sites near the border between Nevada and Utah within the IPCCC. After the field trip, the Tectonics class completed a detailed literature review of the overall tectonic evolution of the region while the Mineralogy students petrographically analyzed the collected samples. This report provides a summary of the results, including mineralogical descriptions; an interpretation of a piece-meal, or piston-like, collapse of the caldera complex; and a connection between the local geology and the regional tectonic setting.

KEY WORDS: Basin and Range tectonic province, ignimbrites, Sevier Orogeny, Laramide Orogeny, Farallon Plate, Cordilleran Orogeny, Nevadaplano, super volcano

INTRODUCTION

In early September 2015, the Southern Utah University geology program organized a field study to investigate two sites: Condor and English Canyons. The sites pertain to the Indian Peak-Caliente Caldera Complex (IPCCC) in eastern Nevada and are believed to be the source of some of the largest eruptions ever known in Earth's history (Best *et al*., 1993). Both sites are situated approximately 40 km west of the Utah-Nevada border near the town of Caliente, Nevada **(**fig. 1**).**

The objective of the field trip was to better understand how the regional tectonic events influenced the local structural geology and mineralogy, and to describe the expression of that relationship at the outcrop scale in Condor and English Canyons. The results advance our understanding of regional tectonic events, in particular slab subduction and roll-back, and their influence on consequent volcanic eruptive history and chemistry. Considering that the eruptions from the IPCCC were among the largest in Earth's history, and coupled with the fact that densely populated segments of the Pacific Ring of Fire are undergoing analogous events, understanding the relationship between slab-subduction, roll-back, and its consequences is vital indeed.

The two studied sites, Condor and English Canyons, are situated on the eastern margin of the Basin and Range tectonic province at elevations of 1550 m and 1400 m, respectively. The climate is essentially that of a desert, falling under the Koppen climate classification system as a Cold Semi-Arid (BSk) climate. Summers are hot and winters cold, with most of the 225 mm of average annual precipitation falling primarily in the winter (NOAA, 2010). As a result, vegetation is minimal and outcrops are typically well exposed.

The canyons and local surroundings exhibit characteristics typical of the Basin and Range Province: approximately north-south oriented graben-type valleys, bounded on either side by mountains uplifted by normal faults as a consequence of ongoing regional crustal extension.

On a more local scale, despite their close association spatially and temporally, the geology of Condor Canyon is appreciably different than that of English Canyon. Condor Canyon lies outside the caldera and is characterized by relatively simple geology, with numerous layers of ignimbrites varying from several meters to hundreds of meters thick and dipping E-SE. Most of the ignimbrites are at least moderately indurated and do not contain large fractions of pumice or clasts, with a few exceptions. The ignimbrites do vary appreciably, however, in regards to color, phenocrysts visible in hand-sample, vesicularity, and the presence or absence of vitrophyres. English Canyon, conversely, is situated on the margin of the caldera and is more complex geologically.

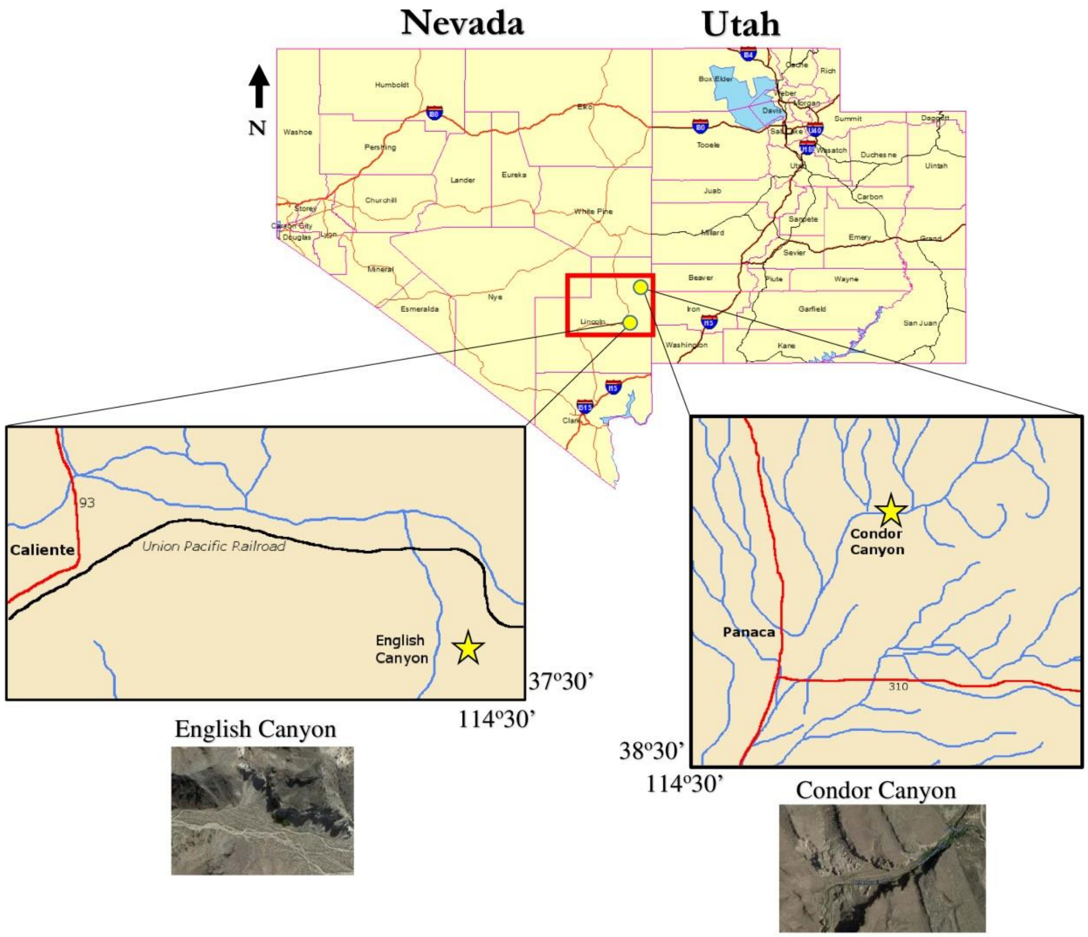

Figure 1. The Indian Peak-Caliente Caldera Complex located in southeastern Nevada. Condor Canyon is located in the northern part of the red rectangle, and English Canyon is in the southeast part of the same rectangle. Both sites are approximately 40 km west of the Utah-Nevada border.

The west-facing outcrop in English Canyon exposes a commonly altered basal block and ash layer with varied clast sizes and roundedness and a minimum thickness of 6 m. The clasts largely consist of welded ignimbrites, shown at the base of the photo in Figure 2. Above this layer lies a thick, off-white to tan colored volcaniclastic siltstone that displays numerous depositional structures such as ripple marks, fining-upwards sequences, and mud cracks, as well as dm-scale soft-sediment folding. Portions of the layer have weathered in planar sheets of variable thickness, also visible in Figure 2. There are also several faults visible at the outcrop with offsets ranging from cm- to m-scale. Observations and sample analyses from the two canyons led to this report's interpretation that the Caliente Caldera collapsed in a piecemeal, piston-like, manner. English Canyon records the events that occurred at the caldera rim, and Condor Canyon records ignimbrite deposition immediately outside of the caldera. This report describes the broad tectonic setting, the outcrop-scale geology at each canyon, and the mineralogical analyses that contributed to this interpretation.

Figure 2. Block and ash unit below, and layered volcaniclastic deposits stratigraphically above. The block and ash layer has an ashy matrix and a high concentration of phenocrysts and clasts. The majority of the clasts are brown and red with quartz, plagioclase, and amphibole. The matrix has sand-to-silt-sized grains that are tan colored. The thickness of this layer varies from no visible outcrop to 6 m, but the base is not exposed. The layered volcaniclastic deposits stratigraphically above contain layers ranging from less than 1 cm to 3 cm. The unit is approximately 10-20 m thick.

TECTONIC SETTING

Evolution of the Farallon Plate Subduction

The Phanerozoic history of western North America has been controlled by the evolution of the Farallon Plate (fig. 3). Around 200 million years ago, Pangea was beginning to pull apart into the modern continental arrangement. The easternmost part of the present day North American continent evolved into a passive rift margin. The western part of the North American continental crust, however, began to grow through accretion of terranes carried by the subducting Farallon Plate.

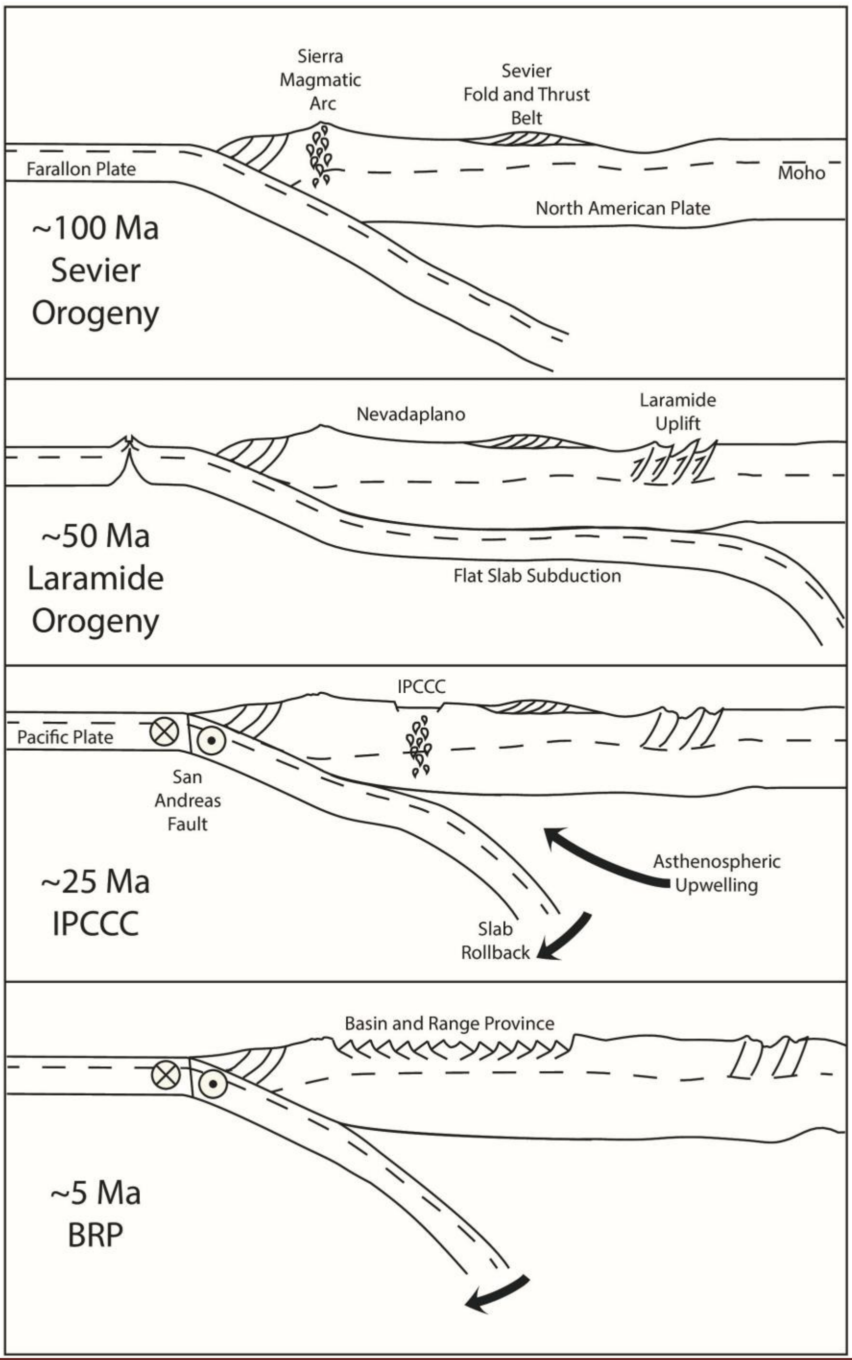

Figure 3. Subduction history of the Farallon Plate. At about 100 Ma the subduction angle was typical with volcanism present. At about 50 Ma the angle flattened, marking a hiatus in volcanism. At about 25 Ma the slab was rolling back, which generated a higher than normal magma influx. At about 5 Ma volcanism had ceased, and extension was the dominant tectonic process. This cross-section view shows the Nevadaplano stretching from the Sevier Mountains to the foreland basin (Best *et al.*, 2013).

A subduction zone formed on the west coast of North America in the late Mesozoic, but its origin is unknown. The dense oceanic Farallon Plate and the North American continental crust started to converge at about 200 Ma. The first evidence of major terrane accretion dates back to around 160 Ma (Sigloch, 2013). The Farallon Plate was subducted continuously under the North American plate at a typical subduction angle of approximately 45 degrees. This resulted in the thin-skinned foreland fold-and-thrust belt of the Sevier Orogeny. Over time, the angle of subduction decreased dramatically, which led to the thick-skinned basement-cored uplifts of the Laramide Orogeny. The contractional history of the region is described in more detail in the following section.

Hotspot activity likely formed the volcanic arcs in the northern Farallon that were among the first of the accreted terranes to collide with North America around 165 to 155 Ma (Chapin, 2014). Accretion continued, and at around 125 Ma a large archipelago collided with North America causing severe deformation and tilting as well as increased volcanism (Symons, 2008). Magmatic belts continued to collide with North America for the next 35-40 Ma during the apex of the Sevier Orogeny. At approximately 85 Ma, the Laramide Orogeny began, which overlapped the Sevier Orogeny in both time and space. The last known terrane accretion occurred at approximately 50 Ma, overriding previous minor accretions and creating more volcanism in the area (Goes, 2013).

Plate subduction continued after this until about 37 Ma when the Farallon Plate under the North American Plate began to rollback, forming the calderas studied in this paper by allowing hot asthenosphere to rise between the subducted plate and the continental crust (Chapin, 2013). This rise of asthenosphere caused increased volcanism as the hotter and less dense molten rock made its way to the surface through faults and other weaknesses. The following sections describe the contractional, extensional, and volcanic histories of the region.

Contractional History of the Southwest

During the late Jurassic, most of the southwestern United States experienced little tectonic activity. The Cordilleran Orogeny began near the end of the Jurassic, creating high topography in western North America (Decelles, 2004). The Cordilleran Orogeny reached its peak of activity around 100-90 Ma and consisted of many orogenies, the main ones being the Sevier and Laramide orogenies (Dilek and Moores, 1999). During the time of the Cordilleran, the crust in the southwestern United States underwent intense thickening. At this time the crust reached thicknesses of up to 55-65 km due to Sevier Orogeny contraction (Chapman *et al.*, 2015).

As this contraction thickened the plate, it created a large highland known as the Nevadaplano (fig. 3) (Henry *et al.*, 2012). The highland itself was 5-6 km above sea level and covered an area from the Sevier fold-and-thrust belt to a massive foreland basin (Best *et al.*, 2013). Rivers flowed to the east across the highland and transported sediments into the foreland basin. These deposited sediments are part of the remaining evidence of the existence of the Nevadaplano (Dilek and Moores, 1999).

Other evidence suggesting the existence of the Nevadaplano comes from metamorphosed rock. As the contraction from the Sevier Orogeny created the Nevadaplano, extreme pressures in the base of the highland caused the sedimentary rock of the crust to metamorphose. Today these rocks have been exposed by erosion, providing evidence of the Nevadaplano (Decelles, 2004).

Around 50 Ma the contraction from the Sevier Orogeny began to subside, which has been attributed to a shallower angle of subduction of the Farallon Plate (Rahl *et al.*, 2002). The flat-slab subduction led to the end of thin-skinned deformation and initiated the thick-skinned deformation of the Laramide Orogeny primarily to the east of the Sevier (Armstrong, 1968). Large basement-cored uplifts contributed to the final stages of crustal thickening before the subducted Farallon slab began to roll back, marking the transition from contraction to extension in the American Southwest (Rahl *et al.*, 2002).

Extensional History of the Southwest

In western North America, normal faults spaced 20-30 km apart created linear mountain ranges and basins oriented north-south, known as the Basin and Range (Egger and Miller, 2011). Zones of extension span north into Canada, south into Mexico, west into California, and east into Utah, Montana, and New Mexico (Sonder and Jones, 1999). The main portion of the extended crust is visible in Figure 4. According to Egger and Miller (2011), the Basin and Range is bounded to the west by the unextended Sierra Nevada and to the east by the Colorado Plateau. Dickinson (2006) made the distinction that the Basin and Range taphrogen, the portion of the crust that has experienced extension, extends from the Pacific Northwest to Mexico, but the Basin and Range region itself is located primarily in Nevada and Utah.

The Basin and Range can be divided into northern, central, and southern sections (Sonder and Jones, 1999). The northern section has the highest heat flow, highest elevation, and thinnest crust. The southern portion has the lowest heat flow, lowest elevation, and least tectonic activity. The central portion has characteristics that are intermediate between the northern and southern portions of the Basin and Range. Parts of the central and northern zones have extended by about 250±50 km, which is about 250% extension (Sonder and Jones, 1999). However, the amount of extension varies greatly, and the average extension throughout the Basin and Range is between 50% and 100% (Parsons, 1995; Sonder and Jones, 1999).

The initiation of faulting occurred in discrete locations at different times (e.g. Sonder and Jones, 1999; Egger and Miller, 2001; Colgan *et al.*, 2006). The northern Basin and Range extension began between 55 and 40 Ma, the central Basin and Range extension began around 25 Ma, and the southern Basin and Range extension began around 16 to 14 Ma (Sonder and Jones, 1999).

Figure 4. Basin and Range province, modified from USGS (2014) and Dickinson (2006). The Basin and Range region is shown here in gray. The red polygons outline this study's field areas: English and Condor canyons. The Basin and Range region in North America has extended an average of 50% to 100% since 55 to 44 Ma (Parsons, 1995; Sonder and Jones, 1999). Most extension occurred in the Basin and Range region shown here, but areas undergoing extension continue southward into Mexico and northward into Canada (Dickinson, 2006).

The models that aim to explain what drove the extension of the Basin and Range have varying strengths and weaknesses. It is likely that many of the models are correct to some degree, and a combination of many models must be used to fully understand Basin and Range extension (Sonder and Jones, 1999). Some of these models include shear forces originating from the San Andreas Fault (Sonder and Jones, 1999;

Dickinson, 2006) and the transfer of tension from the northbound Pacific plate through the Farallon plate and into the North American plate (Sonder and Jones, 1999). One model explaining Basin and Range extension involves the collapse of the raised Basin and Range after its confining forces were reduced (Parsons, 1995). The subduction of the Farallon plate beneath North America caused compressional stresses that raised the Nevadaplano (Parsons, 1995). The raised Nevadaplano therefore had a significant amount of potential energy due to its height. When the compressional forces from the Farallon plate subduction were lessened, the potential energy contained in the Nevadaplano due to its height became greater than the stresses that were compressing the region. The potential energy resulting from the increased crustal height was released as the region thinned vertically and extended laterally, approaching isostatic equilibrium (Parsons, 1995). Perhaps the processes described in this model combined with the increased temperature due to asthenospheric upwelling during slab rollback both contributed to the transition from contraction to extension.

The crustal thickness of the Basin and Range before extension was similar to the current Rocky Mountains and Colorado Plateau thickness. One may wonder why these heightened regions were not incorporated into Basin and Range extension if they were also subject to tension forces created from the collapse of the uplifted continent after the continents confining forces were reduced. According to Parsons (1995), ignimbrites (perhaps including those involved in the Indian Peak Caliente Caldera Complex) were placed in the Basin and Range at the onset of extension, heating the region and making the region more ductile and susceptible to flow. This may have allowed the Basin and Range to extend while other raised parts of North America did not (Parsons, 1995). Sonder and Jones (1999) discussed a model that is consistent with this, describing how some of the Basin and Range may have extended due to destabilization of the lithospheric mantle beneath the northern Basin and Range. The destabilized lithospheric mantle began heating up the upper lithosphere, causing the upper lithosphere to become more buoyant. This buoyancy, coupled with the hotter and less viscous lithospheric mantle, allowed for easy extension of the uplifted northern Basin and Range. The destabilization of the lithospheric mantle and magmatic activity beneath the Basin and Range may have been a consequence of the roll-back of the Farallon Plate (Best *et al.*, 2013).

Supervolcano Development

While many questions surround the relationship between subduction and supervolcano development, the key elements to supervolcano development seem to be pronounced crustal shortening combined with an increased geothermal gradient and/or magma influx (Best *et al.*, 2013; Maughan *et al.*, 2002; Salisbury *et al.*, 2010; de Silva 1989; de Silva, 2008). Currently, studies relating to these very large eruptions are being conducted in the central Andes of South America, New Zealand, and Indonesia (de Silva, 2008; Salisbury *et al.*, 2010; de Silva, 1989). Of these volcano-tectonic settings, the Altiplano-Puna Volcanic

Complex (APVC) in the central Andes represents the most accurate modern analog to the Great Basin volcanics. The Altiplano-Puna plateau is second only to the Tibetan Plateau in terms of areal extent, elevation, and crustal thickness, currently about 70 km thick (Salisbury *et al.*, 2010). This location is unique in that this thickened crust is also associated with subduction related magmatism, as was the case in the IPCCC during the Oligocene and Miocene in North America.

Supervolcano development in the IPCCC is a result of several interacting volcano-tectonic processes. As described above, the fundamental process to this setting is the subduction of the Farallon Plate beneath the North American Plate. This subduction process created over-thickened continental crust (about 70 km) similar to the APVC today (Best *et al.*, 2013; Maughan *et al.*, 2002; Salisbury *et al.*, 2010; de Silva 1989; de Silva, 2008). It is thought that the heat generator for the APVC is the delamination of the lithosphere which brings hot asthenospheric material into contact with hydrated crust, inducing melting (de Silva, 1989; Salisbury *et al.*, 2010). Similarly, the proposed heat generator for the IPCCC is slab rollback of the Farallon Plate (Fig. 3) (Best *et al.*, 2013; Maughan *et al.*, 2002; Smith *et al.*, 2014). Evidence for this slab rollback is seen in the southwestward sweep of magmatism across the region along with the paleogeographic record of stream capture and lake system evolution (fig. 5) (Smith *et al.*, 2014; Best *et al.*, 2013).

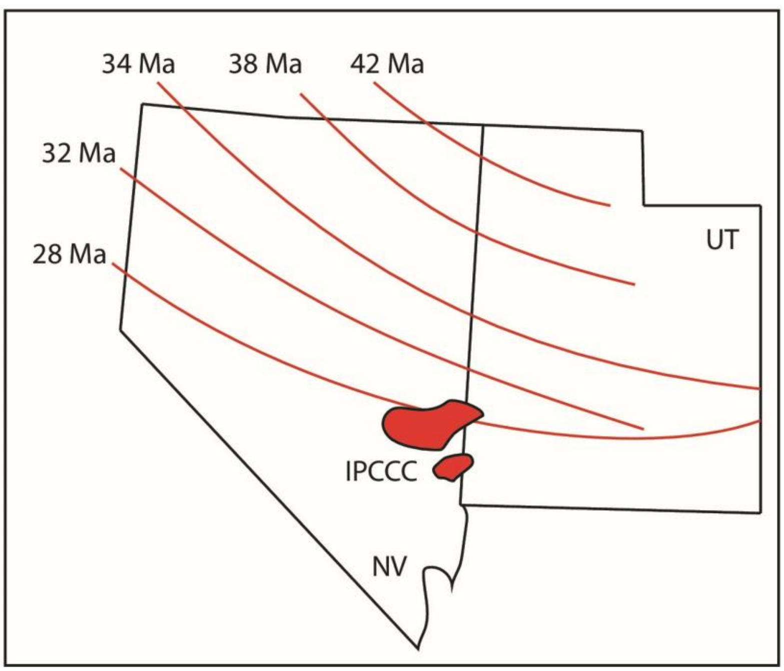

Figure 5. Southwestward sweep of magmatism across the Great Basin region. The sweeping magmatism is thought to follow the rollback of the Farallon plate beneath the North American Plate with the oldest volcanics farthest from the plate boundary and youngest nearer the plate boundary.

The IPCCC monotonous ignimbrite eruptions occurred at about 36-18 Ma. It is very likely that the lower and middle crust temperatures were elevated with respect to the normal geothermal gradient (Maughan *et al.*, 2002; Salisbury *et al.*, 2010; de Silva, 1989). Elevated geothermal gradients and elevated crustal temperatures coupled with increased mafic magma input greatly aid in the assimilation of the surrounding crust (Maughan *et al.*, 2002; Salisbury *et al.*, 2010; de Silva, 1989). This thickened crust accommodated large areas of pooled magma at varying depths within the crust (fig. 6). The thickened crust and pooled magma acted as a crustal filter, resulting in large-volume dacite eruptions comprised of plagioclase, biotite, amphibole, quartz, and sanidine. The specific eruption products of the IPCCC were studied in hand samples as a part of this project.

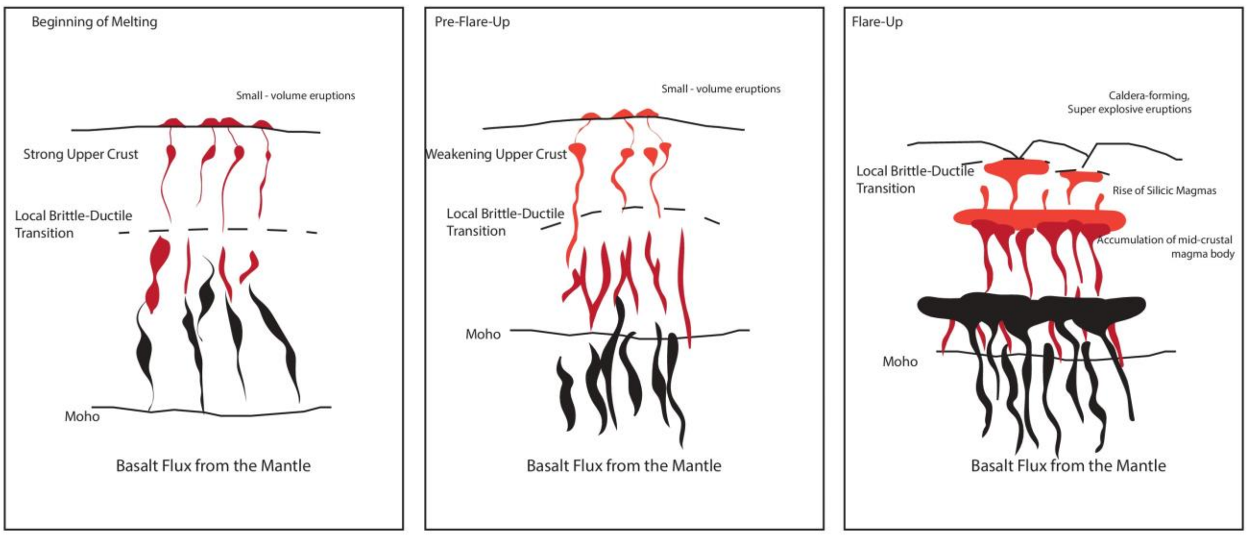

Figure 6. Stages of melting leading to flare-up conditions (modified from de Silva *et al.*, 2006). As the magma system evolves through time, the conditions within the crust become more favorable to supervolcanic eruptions. Pooled magmas in sill shaped chambers prevent the migration of less evolved magmas while also incorporating large amounts of crustal material, giving rise to large volumes of silicic magma. These large volumes of silicic magmas are then erupted, resulting in the large ignimbrite deposits, similar to those seen in English and Condor canyons.

FIELD METHODS

For both canyons, five teams of three to four people each were formed to collect structural and mineralogical field data. Teams completed transects of the canyons, taking notes and samples along the way. Each team defined their own stratigraphy based upon their observations, with the understanding that the collating of data would take place post-field trip. Structural data and sample locations were chosen based upon the presence of features of interest, including but not limited to contacts, faults, changes in the rock fabric or texture, and features such as ripple marks or upwards-fining sequences.

Teams collected structural data (strikes and dips) using Brunton field compasses. Observations and photos/sketches were also made to describe the nature of the layering, lithologies, and structures. As the outcrops were relatively accessible, hand-samples were gathered directly from the outcrop as opposed to the float, so as to avoid ambiguity regarding the actual source, and to obtain a fresh and unweathered surface to observe. Target size was 7–8 cm, allowing for several thin sections to be made from a single sample if necessary, but still preserving enough material to be useful as a hand-sample. An initial assessment of modal abundances in the hand samples was also performed at this time.

Upon completion of data collection at both canyons, a group meeting was held in the field to discuss a probable sequence of events. The following sequence was unanimously as being the most probable: Farallon plate subduction and slab roll-back, the appearance of caldera-complexes and related deposits, collapse of the caldera-complexes and cessation of volcanic activity, and then Basin-and-Range extension. This effectively concluded the field trip, and upon return to campus, all the field notes were collated and the production of thin sections began, where more accurate measurements and finer analyses were made.

LAB METHODS

The rock samples from the determined units in the field were petrographically analyzed. First, a 1-cm-thick cross section was cut from each hand sample then cut to fit on standard 27 x 46-mm glass slides. Each billet was cemented onto a glass slide with epoxy. The mounted samples were further cut on a small saw and ground down on to less than 1 mm thick, then hand polished/ground to 30 µm thick using 600 grit polishing compound. The thin sections were used to help identify the mineral content, determine modal abundances, and observe compositional features in the layers.

RESULTS

The following datum is based upon observations made on September 16 and 17, 2015. Condor Canyon was divided into six layers based on similar crystal and lithic contents as well as structural characteristics observed at the outcrop scale. Layers are labeled A-G, A being the oldest exposed layer as shown in Figure 7. The layers in Condor Canyon are all conformable with very similar strikes and dips of N30°W, 20°NE respectively.

English Canyon, which is located 32 km from Condor Canyon, shows dramatically different structural and lithologic properties (fig. 8). The units of English Canyon are highly faulted and display multiple volcanic and sedimentary structures. The lithologic descriptions are both Condor and English Canyons are presented here.

Condor Canyon

Layer A (14 m thick) is a highly weathered layer with conjugate fractures throughout the rock body. It is not strongly indurated and contains 25-50% poorly to mildly sorted lithic fragments and pumice. The rock layer has an ashy light gray to light brown color. Layer A is not strongly compacted, and consists of a light-grey to light-brown matrix (50% of the rock body) with variable vesicularity. Hand-samples are highly clastic (40%) with clasts that are typically white, pink, or black, poorly sorted, and are variable in terms of roundness, and composition. Most clasts consist of either pumice or ignimbrites, and are between 1–5 mm in size, though significantly larger clasts are common throughout the rock body. However, due to the various sizes (10-30 cm), it is difficult to get an accurate representation of these larger clasts. Among the non-matrix material, samples are rich in clasts including pumice (70–80% of non-matrix material, and 10% of entire rock body). Quartz (95%) is the most abundant mineral in the phenocrysts typically forming irregular masses or easily visible crystals up to 3 mm in size. Plagioclase (3%), amphiboles (1%), and biotite (1%) are present in very small quantities.

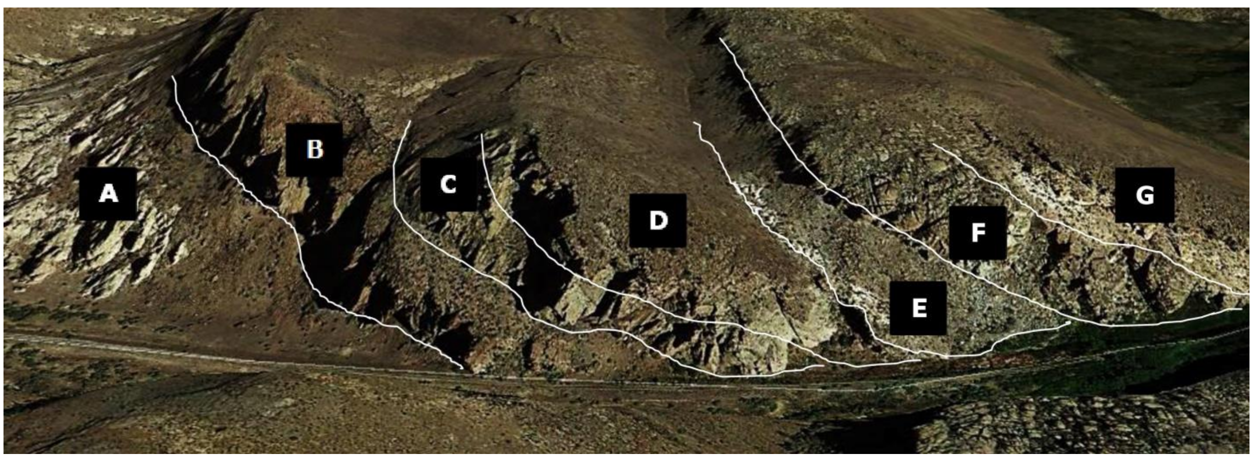

Figure 7. A Google Earth image of Condor Canyon with boundary lines superimposed on layers A-G as defined by study. View is to the north. Layer A is the oldest ignimbrite in the outcrop to the west (left), and layer G is the youngest to the east (right) of the canyon. Boundaries were placed based on lithologic and structural differences observed in the field.

Layer B is 33 m thick and includes a vitrophyre at the bottom 2-3 m. Stratigraphically above the vitrophyre, the rock becomes more vesicular in texture. The color of the matrix changes from black at the base to light brown, grey and purple, then darker shades of brown, red, and purple at the top. Reverse polarity was observed with a compass caused by this iron-rich layer. Layer B is very brittle and friable. It also shows prominent vertical jointing in both the vitrophyre and the upper portion of the ignimbrite. The upper and basal portions have strong competency, while the middle section is less competent, more smoothly weathered, and less blocky. Layer B is a densely welded unit. Vesicularity is variable from the base to the top of the unit. Phenocrysts (25-30% of the rock body) and pumice inclusions (10%) also increase in size and frequency higher in the profile. The unit has a phenocryst composition of amphibole (40%), plagioclase (40%), quartz (10%), and biotite (10%). Flow alignment is present (fig. 9). A vitrophyre (2 m thick) makes up the base of the unit. The vitrophyre has magnetic properties, indicated by interfering with compasses within 3-5 m. The vitrophyre is moderately crystal rich (15-20%), composed of plagioclase (75%), quartz (10%), amphibole (10%), and biotite (5%). Either flow alignment or crystal alignment caused from compression is present (fig. 9). Excluding the vitrophyre, the entire layer has flattened fiamme inclusions that are on average 10 cm long and 3 cm thick. Clasts are present in the supra-vitrapheric section that make up 5% of the rock and have an average size of 1-10 mm.

Figure 8. Overview of English Canyon. The cliffs surrounding English Canyon show the separation of the volcaniclastic layer and the block and ash layer. The volcaniclastic layer is off-white and tan in color. The block and ash layer, stratigraphically below the ash layer, is dark gray. On average, the volcaniclastic layer is triple the thickness of the block and ash layer exposures. A more detailed view of the two layers and their contact is shown in Figure 2.

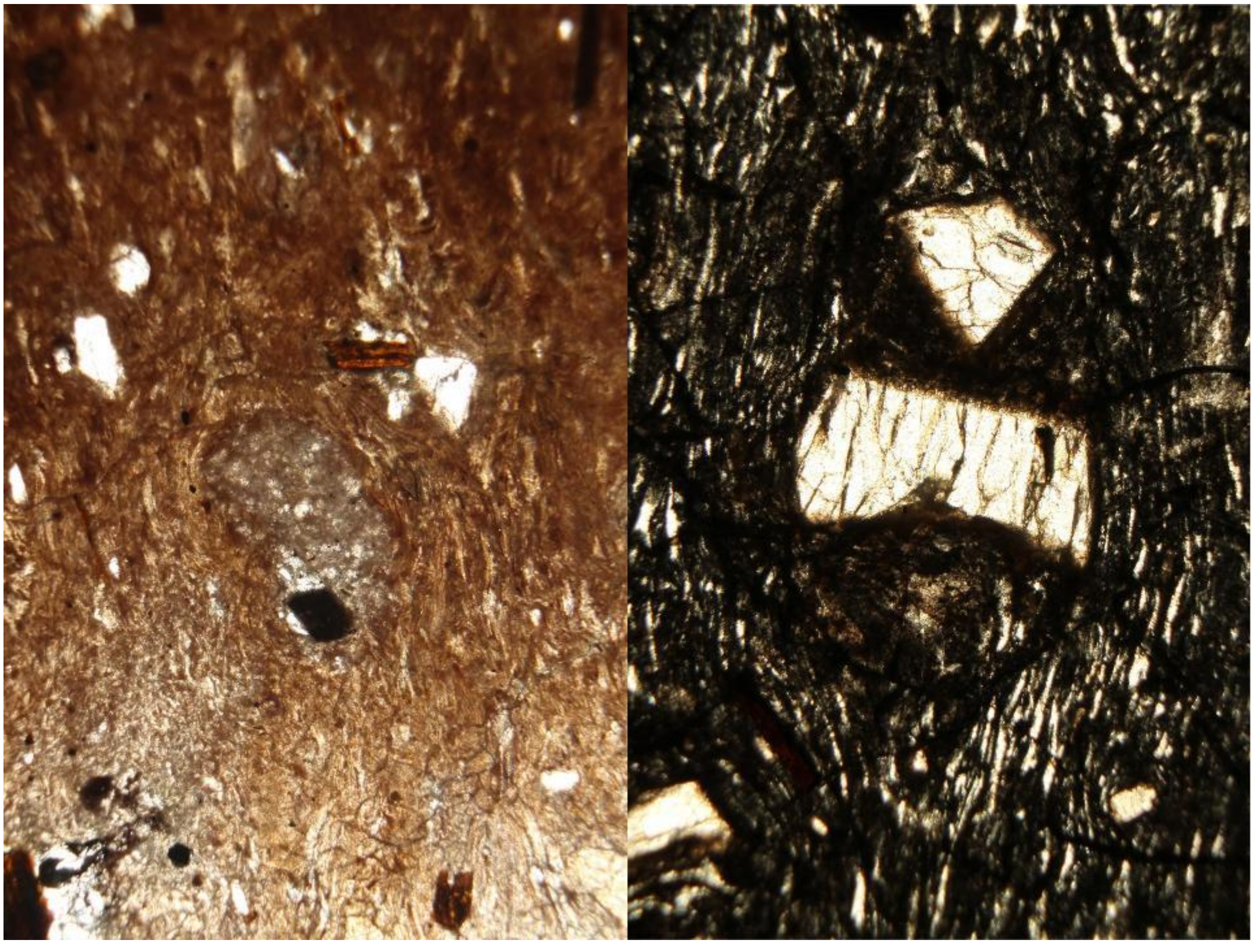

Figure 9. Example photomicrographs, both made from unit B (a volcanic rock unit in Condor Canyon). The left picture shows the unaltered portion of unit B in normal polarized light. The grains show flow alignment. The right picture shows the vitrophyre of unit B in normal polarized light, which shows the orientation of grains that probably occurred as a consequence of compression.

Layer C forms a 15-20-m cliff face. The bottom of this layer is a 5-m-thick vitrophyre. There is a 0.5-1.0-m zone of the vitrophyre that contains scattered lithophysae (30-50 cm in diameter). The unit shows a repeating pattern of matrix alteration, alternating from red to gray a total of three times in the unit. This layer becomes more vesicular and less indurated moving upwards from the vitrophyre. The pattern explained above of the reddish rock (bleaching and increasing vesicularity) repeats two more times in sequence in this layer. The vitrophyre is phenocryst rich (45%) composed of plagioclase (60%), quartz (30%), amphibole (7%), and biotite (3%). The main body of Layer C is phenocryst poor (10-15%), composed mainly of altered amphiboles (60%), plagioclase (35%), and biotite (5%) decreasing in occurrence further up from the vitrophyre. Crushed pumice (possible fiamme, 5% of rock mass) inclusions of various sizes (.3-3 cm) increase in occurrence further up from the vitrophyre.

Layer D is significantly thicker (25-30 m) compared to all other layers. There are flow structures near the bottom of the layer. Layer D's matrix has a light red to grey and brown color and there are conjugate fractures within the rock body. Layer D has a brown and red fine matrix. There are no lithic fragments in the hand samples. The rock contains phenocrysts (35%) and some fiamme (2%). The phenocrysts contain plagioclase (60%), amphibole (30%), quartz (7%), and biotite (3%). The quartz and feldspar phenocrysts are typically about 2 mm and the other phenocrysts are typically about 0.25 mm.

Layer E is not very competent and breaks easily. The matrix is very fine and ashy. Large phenocrysts are present in the majority of this rock. Being very friable, this layer crumbles when handled. Layer E has some compaction that is shown by visible, thin layers. Phenocrysts (60%) make up a large percentage of the total structure of the rock. Within the phenocrysts are plagioclase (45%), quartz (25%), amphibole (25%), and biotite (<5%). The quartz content is partially secondary quartz.

Layer F is a dark gray colored rock unit with a high abundance of phenocrysts and mineral content in the rock make-up. Layer F is relatively thicker than its surrounding layers, and more competent as well. Layer F has a large phenocryst composition (60%) of ignimbrite body. Within the phenocrysts are plagioclase (60%), amphibole (35%), biotite (5%), and some samples had the presence of quartz (<1%).

Layer G's matrix ranges in color from intermediate to felsic and black to pink/red. It is vertically fractured with pumice clasts. There is highly weathered pumice and secondary quartz on some surfaces. The majority of the layer is fine-grained with some mineral clasts and trace lithics towards the bottom of the segment. It is not particularly well indurated. Layer G has a gray and purple matrix with some fiamme (5%) in the composition. This material is welded, well sorted, and poorly rounded. Phenocrysts (25%) in the sample consist of amphibole (53%), plagioclase (45%), biotite (1%), and quartz (1%).

English Canyon

In English Canyon, the rock units are significantly complicated by abundant faulting. One of the heavily faulted units is a block and ash flow (fig. 2). This area is defined by ashy material with brown, red, and tan blocks of lithics of varying sizes throughout the entirety of the section. The blocks range from 10 cm to 50 cm. The thickness of the unit varies with areas that are not visible and others up to 6 m. The unit is fairly well indurated, but also heavily fractured. Much of the unit is covered in weathering product.

The volcaniclastic unit stratigraphically above the block and ash unit is large compared to the block and ash unit at thicknesses of 10-20 m (fig. 8). The unit is an ashy color with variable grain sizes in the varying areas. There is a prevalence of thin, laminated layers that have fining upwards sequences. These layers are dramatically folded in some areas. There are some structures found in the ashy volcaniclastic unit and at the division between that unit and the block and ash unit. Ripple marks were present in the thin, compacted ash layers and some blocks from the block and ash unit were included in the lower portion of the ashy segment.

The block and ash unit from English Canyon is poorly sorted with an ashy matrix. It is tan colored and composed of sand/silt sized grains. There are phenocrysts between 2 and 15 cm (30%) and between 2 and 20 mm (10%). The clasts are typically brown/red but are often covered in light tan colored sediment. The phenocrysts consist of amphibole (30%), quartz (20%), and plagioclase (20%). 30% of the mineral composition is highly altered. The crystals within the clasts are typically about 1 mm (Table 1).

Layer	Matrix	Fiamme and Pumice	Phenocrysts	Quartz	Amphibole	Plagioclase	Biotite
A	50	10	40	95	1	3	1
B (Vitrophyre)	80-85	30	15-20	10	10	75	5
B	70-75	10	25-30	10	40	40	10
C (Vitrophyre)	55	0	45	30	7	60	3
C	80-85	5	10- 15	0	60	35	5
D	63	2	35	7	30	60	3
E	40	0	60	25	25	45	<5
F	40	0	60	<1	35	60	5
G	70	5	25	1	53	45	1
Block and Ash	50	0	40	20	30	20	0

Table 1. A comparative representation of modal abundances from collected mineralogical data of units A-G from Condor Canyon and the block and ash unit from English Canyon.

DISCUSSION

As described above, the evolution of the subduction of the Farallon plate contributed to the creation of the IPCCC. In the slab-rollback model, the abundant intermediate to felsic ignimbrite deposits were produced by the slow rise of magma, generated by asthenospheric upwelling through a lithosphere already thickened from the contraction of the Cordilleran Orogeny. This additional thickness gave the rising magma ample opportunity to become enriched in silica, resulting in the felsic and intermediate deposits we have seen. The silicic magma would also contribute to the size of the eruptions and ensuing caldera collapses, which are integral to the sedimentary-style deposition that has been noted.

We have developed a model reflecting how the observed geological features described above, including asymmetrical ripple marks, desiccation cracks, laminations, rip-up clasts, and outcrop-scale faults, could have formed due to the piecemeal collapse of the Caliente Caldera. In this model, the caldera does not collapse in one large block, but breaks into many smaller pieces which fall at differing times (fig. 10). This causes a disparity in the heights of the layers and influences the rate and placement of following ignimbrite deposition. This explains both the varying thicknesses of block and ash deposits within English Canyon through their being deposited into basins of varying depths and the faulting found within the layers through the further movement of pistons after deposition has occurred.

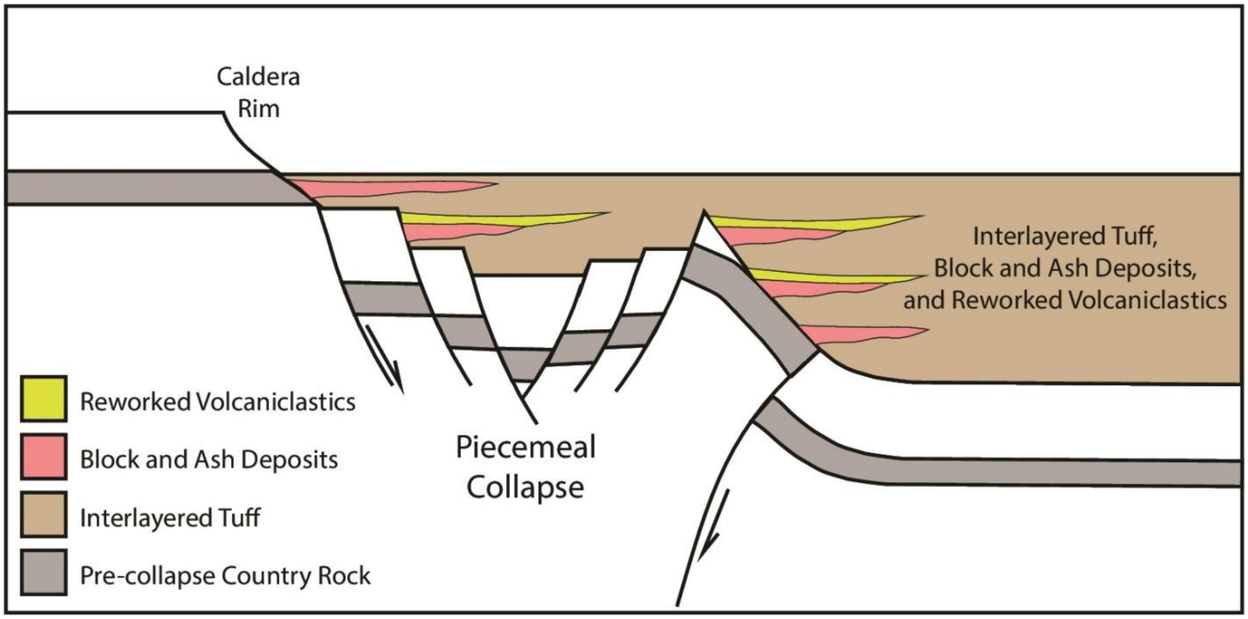

Figure 10. Model of a piecemeal collapse such as interpreted in English Canyon. Note the heavily faulted underlying rock and the block and ash deposits (shown in pink). Unlike the figure, however, the faulting in English Canyon can be seen throughout the block and ash deposits on an outcrop scale, but this can be explained by the speed of the layer's deposition having outpaced the caldera collapse.

In the case of such a large supervolcano, it is far from unreasonable to assume that the ensuing collapse would create a basin, entrapping streams and runoff from a vast portion of the surrounding area and causing the sedimentary processes necessary to create the deposits mentioned above. The existence of several large faults cutting through the block and ash layers in English Canyon support the piecemeal or piston-like collapse model. These faults exemplify the piecemeal collapse model through their extreme variations in height within the layer, showing that the portions of caldera below them had fallen at differing speeds after the eruption of the volcano and deposition of the ignimbrite complexes. Such block and ash deposits on the edges of caldera-related faults are interpreted as wall collapse breccias.

A collapse as described above, with portions falling at different times creating sudden changes in the angle of the surface, would create the potential energy needed for high-energy fluvial systems. Evidence that this was indeed the case includes the rip-up clasts observed on the lower layers, where large clasts from a lower layer were found to have been included into the ashy matrix of one above. As the energy in these systems began to wane due to the leveling of the caldera pistons through erosion, the rip-up clasts would give way to lower-energy deposits like the asymmetrical ripple marks seen on the upper strata. The fine laminations that were noted on some layers can be depicted as having been deposited by laminar flows, which would require higher energy than the ripple marks mentioned earlier, again pointing to varying energy levels during deposition. Desiccation cracks were also common, and believed to be due to the ash's expansion and contraction upon contact with runoff during wet and dry periods.

The deposits in English and Condor canyons are of interest to us specifically due to their locations within the IPCCC as a whole, being rim (English) and pyroclastic flow (Condor) deposits. These two locations helped us to create a more accurate model of the eruption event as a whole, from explosion to collapse and finally to the deposition of sedimentary-processed volcaniclastic material such as the laminar flows. In researching these canyons, we have also gained accurate and important insight toward understanding the nature of ignimbrites found in the area, both physically and chemically.

ACKNOWLEDGEMENTS

We'd like to thank Brandon Gagnon for providing continued reviews of this manuscript. The writing quality vastly improved due to his efforts.

REFERENCES CITED

Armstrong, Richard Lee., 1968. Sevier Orogenic Belt in Nevada and Utah. *Geological Society of America Bulletin* v. 79 (4) p. 429-458.

Best, M. G., Christiansen, E. H., and Gromme, S., 2013. Introduction: The 36-18 Ma southern Great Basin, USA, ignimbrite province and flareup: swarms of subduction-related supervolcanoes. *Geosphere*, v. 9 (2) p. 260-274.

Best, M. G., Gromme, S., Deino, A. L., Christiansen, E. H., Hart, L. G., and Tingey, D. G., 2013. The 36-18 Ma central Nevada ignimbrite field and calderas, Great Basin, USA: multicyclic super-eruptions. *Geosphere.* v. 9 (6) p. 1562-1636; doi:10.1130/GES00945.1

Best, M.G., Scott, R.B., Rowley, P.D., Swadley, W.C., Anderson, R.E., Gromme, C.S., Harding, A.E., Deino, A.L., Christiansen, E.H., Tingey, D.G., and Sullivan, K.R., 1993. Oligocene-Miocene caldera complexes, ash-flow sheets, and tectonism in the central and southeastern Great Basin. *Field Trip Guidbook for the 1993 Joint Meeting of the Cordilleran/Rocky Mountains Sections of the Geological Society of America*, Department of Geological Sciences, Mackay School of Mines.

Chapin, C., Kelley, S., and Cather, S., 2014. The Rocky Mountain Front, southwestern USA. *Geosphere,* v. 10 (5), p. 1043-1060.

Chapman, J. B., Ducea, M.N., DeCelles, P.G., and Profeta, L., 2015. Tracking changes in crustal thickness during orogenic evolution with Sr/Y; an example from the North American Cordillera. *Geology [Boulder] Pre-Issue Publication.* GeoRef.

Colgan, J.P., Dumitru, T.A., Reiners, P.W., Wooden, J.L., and Miller, E.L., 2006. Cenozoic tectonic evolution of the Basin and Range Province in northwestern Nevada. *American Journal of Science*, v. 306 (8), p. 616-654.

Dickinson, W.R., 2006. Geotectonic evolution of the Great Basin. *Geosphere*, v. 2(7), p. 353-368.

Decelles, P. G., Late Jurassic to Eocene evolution of the Cordilleran Thrust Belt and Foreland Basin System, Western U.S.A. *American Journal of Science*, v. 304 (2), p. 205-68.

De Silva, Shanaka., 2008. Arc Magmatism, Calderas, and Supervolcanoes. *Geology*, v. 36 (8), p. 671-672.

De Silva, S., Zandt, G., Trumbull, R., Viramonte, J. G., Salas, G., and Jemenez, N., 2006. Large ignimbrite eruptions and volcano-tectonic depressions in the central Andes: a thermomechanical perspective. *Geological Society, London, Special Publications*, v. 269 p. 47-63.

De Silva, S. L., 1989. Altiplano-Puna volcanic complex of the central Andes. *Geology*, v. 17, p. 1102-1106.

Dilek, Y., and Moores, E. M., 1999. A Tibetan model for the early Tertiary western United States. *Journal of the Geological Society* v. 156 (5), p. 929-41.

Egger, A. E., and Miller, E.L., 2011. Evolution of the northwestern margin of the Basin and Range; the geology and extensional history of the Warner Range and environs, northeastern California. *Geosphere, v.* 7(3), p. 756-773. doi: 10.1130/GES00720.1.

Henry, C.D., N.H. Hinz, J.E. Faulds, J.P. Colgan, D.A. John, E.R. Brooks, E.J. Cassel, L.J. Garside, D.A. Davis, and S.B. Castor., 2012. Eocene-early Miocene paleotopography of the Sierra Nevada-Great Basin-Nevadaplano Basin based on widespread ash-flow tuffs and paleovalleys. *Geosphere*, v.8 (1), p. 1-27.

Maughan, L. L., Christiansen, E. H., Best, M. G., Gromme, S. C., Deino, A. L. and Tingey, D. G., 2002. The Oligocene Lund Tuff, Great Basin, USA: a very large volume monotonous intermediate. *Journal of Volcanology and Geothermal Research*, v. 113 p. 129-157.

National Oceanic Atmospheric Administration. *1981-2010 Climate Normals for Caliente Nevada*. Retrieved from https://www.ncdc.noaa.gov/cdo-web/datatools/normals

Parsons, T., 1995. The Basin and Range Province. *Continental Rifts: Evolution, Structure and Tectonics*, p. 277-324.

Rahl, Jeffry M., Allen J. Mcgrew, and Kenneth A. Foland., 2002. Transition from contraction to extension in the northeastern Basin and Range: new evidence from the Copper Mountains, Nevada. *The Journal of Geology,* v. 110 (2), p. 179-94.

Salisbury, M. J., Jicha, B. R., de Silva, S. L., Singer, B. S., Jimenez, N. C., and Ort, M. H., 2010. $^{40}Ar/^{39}Ar$ Chronostratigraphy of Altiplano-Puna Volcanic Complex Ignimbrites Reveals the development of a major magmatic province. *Geological Society of America Bulletin*, published online, doi:10.1130/B30280.1

Sigloch, K., and Mihalynuk, M., 2013. Intra-oceanic subduction shaped the assembly of Cordilleran North America. *Nature,* v. 496 (7443), p. 50-56.

Smith, E. M., Carroll, A. R., Jicha, B. R., Cassel E. J., and Scott, J. J., 2014. Paleogeographic record of Eocene Farallon slab rollback beneath western North America. *Geology*, v. 42 (12), p. 1039-1042.

Sonder, L. J., and Jones, C. H., 1999. Western United States extension: how the west was widened. *Annual Review of Earth & Planetary Sciences,* v.27 (1), p. 417.

Symons, D., Smith, T., and Blackburn, W., 2008. Constraining the travels of a "Suspect Terrane: paleomagnetism and geobarometry of two early Cretaceous igneous complexes in the Peninsular Ranges Batholith, California. *Geological Society of America Bulletin,* v. 120 (9-10), p. 1159-1170.

USGS, 2014. Geologic Provinces of the United States: Basin and Range Province: Retrieved from http://geomaps.wr.usgs.gov/parks/province/basinrange.html.